Supplementary Information for

Surface charge modulation boosts electrocatalytic water splitting over iridium catalysts on a polyimide support

Longsheng Zhang,[a] Shouhan Zhang,[a] Jing Bai,[a] Yidan Ding,[a] Jinyu Ye,[b] Yuanhao Song,[a] Elke Debroye,[c] Wei Fan[a] and Tianxi Liu[a]*

[a]*Key Laboratory of Synthetic and Biological Colloids, Ministry of Education, School of Chemical and Material Engineering, Jiangnan University, Wuxi 214122, China.*
E-mail: txliu@jiangnan.edu.cn
[b]*College of Chemistry and Chemical Engineering, Xiamen University, Xiamen 361005, China*
[c]*Department of Chemistry, KU Leuven, Celestijnenlaan 200F, Leuven 3001, Belgium*

Experimental section

Materials

3,4,9,10-Perylenetetracarboxylic dianhydride (PTCDA), p-Phenylenediamine (PDA), IrO_2 catalyst and Nafion (5 wt% in mixture of lower aliphatic alcohols and water) were purchased from Sigma-Aldrich. N-methylpyrrolidone (NMP), ethanol and sulfuric acid (H_2SO_4) were obtained from Sinopharm Chemical Reagent. Carbon nanotube (CNT) dispersion was purchased from Chengdu Organic Chemicals. Carbon paper (HCP-030N) was purchased from Toray Industries. Deionized water was used throughout all experiment. No further treatment and purification were performed in all chemicals.

Preparation of Ir NP@PI catalyst

Polyamic acid (PAA) solution was synthesized from PDA and PTCDA. Firstly, PDA (2 mmol) was dissolved in 15 mL NMP to get a homogenous solution. Then, PTCDA (2 mmol) was added into the mixed solution, which was kept at 220 ℃ for 24 h until viscous PAA solution was obtained. Commercial IrO_2 catalyst (20 mg) was dispersed into PAA solution (240 μL), which was sonicated for 5 min to obtain a homogenous mixture. Then the mixture was heated up in steps in a tube furnace under Ar atmosphere. The temperature nodes were set at 70, 100, 150, 200, 300 and 350 °C. The heating rate was 5 °C min^{-1}. Each temperature node was kept for 2 h to complete the preparation of Ir NP@PI catalyst. Accordingly, a similar procedure without adding PAA was carried out to synthesize the counterpart Ir NP catalyst.

Characterization

The ^1H nuclear magnetic resonance spectroscopy measurements were carried out on a AVANCE III HD 400 MHz spectrometer. The X-ray diffraction measurement was performed on a MiniFlex600 X-ray diffractometer with Cu Kα radiation (λ = 0.1542 nm). The Fourier transform infrared measurements were carried out on a Nicolet 6700 device. The morphological characterization of samples was investigated by using the transmission electron microscopy (JEM-2100plus, JEOL). The X-ray photoelectron spectroscopy (XPS) patterns were collected from a VG ESCALAB 220I-XL device.

The Ir mass loading in the Ir NP@PI sample was evaluated using a thermogravimetry analyzer (TG, Q5000IR, TA Instruments).

Electrochemical measurements

Typically, 5 mg of catalysts and 80 μL of CNT dispersion were added into 500 μL of ethanol with 120 μL of Nafion solution, which was subjected to ultrasonic treatment for 2 h to get a homogeneous ink. The electrochemical measurements were carried out on a three-electrode configuration in 0.5 M H_2SO_4 aqueous electrolyte. Typically, we deposited the catalyst ink on the glass carbon electrode (GCE) to prepare the working electrode. To assess the catalytic activity towards oxygen evolution reactions (OER), stable cyclic voltammetry (CV) scans were achieved by scanning the working electrode from 0.9 to 1.25 V (vs. Ag/AgCl) at a rate of 50 mV s^{-1}. Then, current density versus potential curves were obtained by linear sweep voltammetry (LSV) measurement at a scan rate of 5 mV s^{-1}. All CV and LSV measurements were carried out at 25±3 ℃. In-situ electrochemical impedance spectroscopy (EIS) tests were measured at a potential of 5 mV from 100 KHz to 0.1 Hz. All potentials were referenced to Ag/AgCl electrode and then converted to reversible hydrogen electrode (RHE) by using Equation 1:

$$E_{RHE} = E_{Ag/AgCl} + 0.229 + 0.059 \times pH \quad (1)$$

Electrochemical active surface area (ECSA) calculation

The ECSA of catalysts were calculated based on their electrical double layer capacitor (C_{dl}), which were obtained from CV plots in a narrow non-Faradaic potential window from 0.4 to 0.6 V (vs. Ag/AgCl) for Ir NP@PI and from 0.15 to 0.35 V (vs. Ag/AgCl) for Ir NP. The anodic currents were plotted as a function of scan rate. Then linear fitting was adopted to these points, and the slope of plots gives the value of C_{dl}. The specific capacitance was found to be 35 μF·cm^{-2}, and ECSA values of catalysts were calculated from Equation 2:[1]

$$ECSA = \frac{C_{dl}}{35\ \mu F\ cm^{-2}} cm^2 \quad (2)$$

The specific activity (SA) of catalysts were revealed by normalizing the currents to the ECSA values to exclude the effect of surface area on catalytic performance.

Turnover frequencies (TOF) calculation

The TOF values of catalysts were calculated from Equation 3:

$$TOF = \frac{j \times A}{4 \times F \times n} \quad (3)$$

where j is the current density obtained at 1.53 V (vs. RHE), A is the geometric area, F is the Faraday constant and n is the mole number of active metal atoms *via* Equation 4:

$$n = \frac{m_{loading}}{M_w} \quad (4)$$

where $m_{loading}$ is the loading mass of Ir element, M_w is the molecular weight of active metal atoms. In this work, the mass loading of Ir element for Ir NP@PI and Ir NP samples is based on the results from the TG analysis. The TOF values of Ir NP@PI and Ir NP catalysts were calculated according to the mass loading of active metal atoms.

Mass activity (MA) calculation

The MA values of catalysts were calculated from Equation 5:

$$MA = \frac{j \times A}{m_{loading}} \quad (5)$$

where j is the current density obtained at 1.53 V (vs. RHE), A is the geometric area and $m_{loading}$ is the Ir loading mass based on the TG analysis.

Arrhenius Apparent Activation Energy Determination

The OER kinetics will be increased at elevated temperatures, reflecting the temperature dependence of a chemical rate constant. The apparent electrochemical activation energy (E_a) for water oxidation can be determined using the Arrhenius relationship:[2]

$$\frac{\partial(\log i_k)}{\partial(1/T)}|_\eta = \frac{E_a}{2.3R} \quad (6)$$

where i_k is the kinetic current at overpotential (η) = 300 mV, T is the temperature, and R is the universal gas constant. The Arrhenius plots at η = 300 mV for Ir NP@PI and Ir NP catalysts and controls are shown in Fig. 2e, which reveals a linear dependence on temperature. From the slope of the Arrhenius plot, the E_a can be extracted.

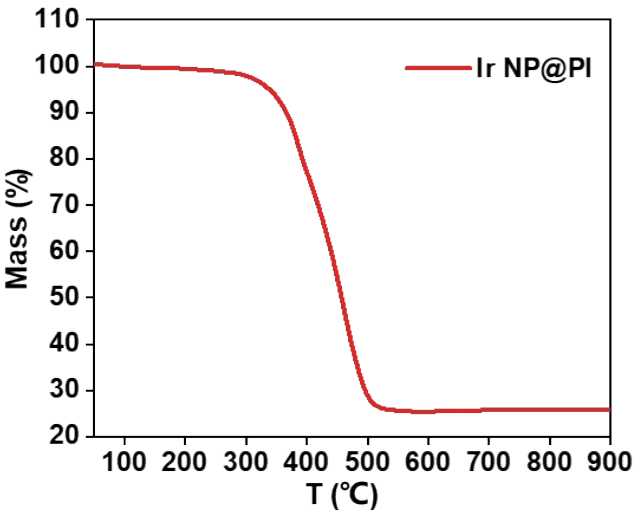

Fig. S1. TG spectra of Ir NP@PI sample.

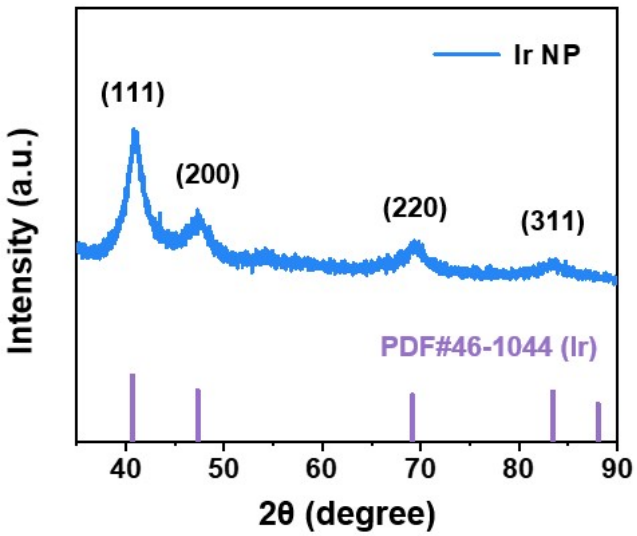

Fig. S2. XRD pattern for Ir NP sample/

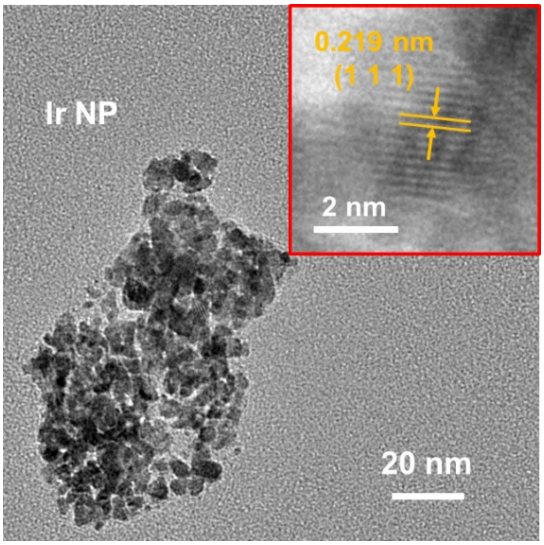

Fig. S3. TEM image for Ir NP sample. Insets is the zoom-in view of TEM mage.

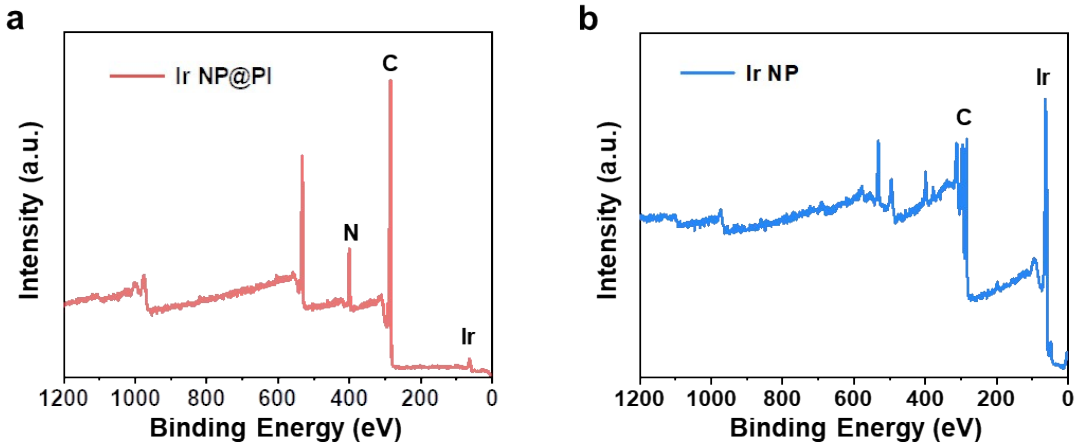

Fig. S4. (a, b) XPS spectra of Ir NP@PI and Ir NP samples, respectively.

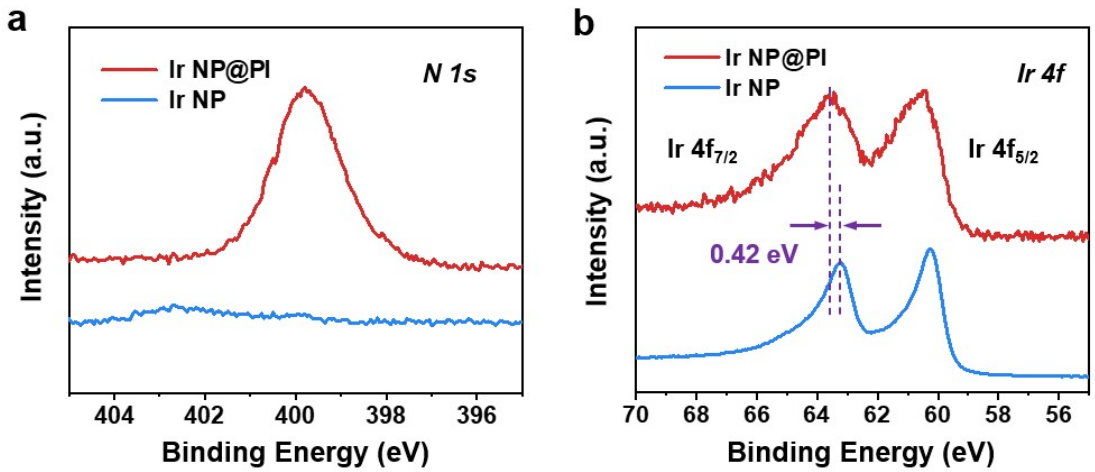

Fig. S5. (a, b) High-resolution XPS N 1s and Ir 4f spectra for Ir NP@PI and Ir NP samples, respectively.

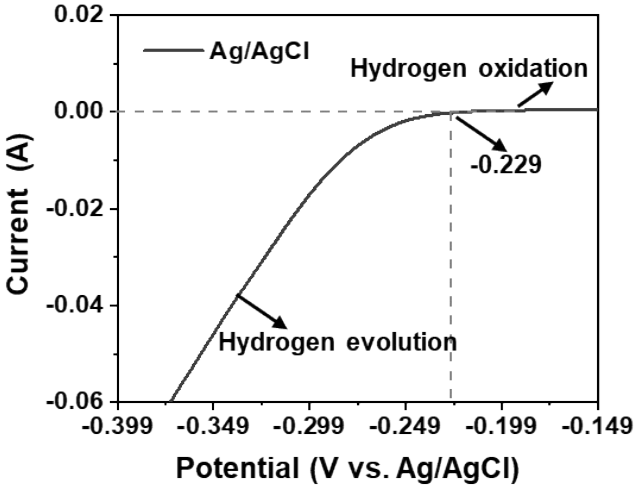

Fig. S6. The calibration curve of Ag/AgCl reference electrode.

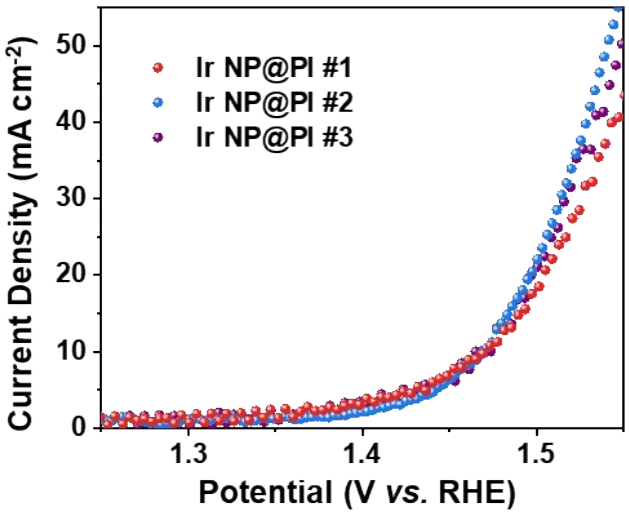

Fig. S7. Three independent LSV tests for Ir NP@PI catalyst measured at a scan rate of 5 mV s^{-1} in 0.5 M H_2SO_4 aqueous electrolyte, respectively. The numbers (#1, #2, #3) denote the results from these three independent LSV tests, respectively.

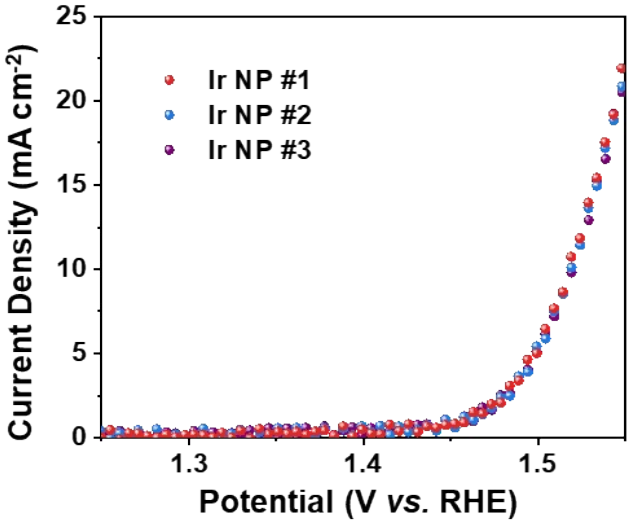

Fig. S8. Three independent LSV tests for Ir NP catalyst measured at a scan rate of 5 mV s^{-1} in 0.5 M H_2SO_4 aqueous electrolyte, respectively. The numbers (#1, #2, #3) denote the results from these three independent LSV tests, respectively.

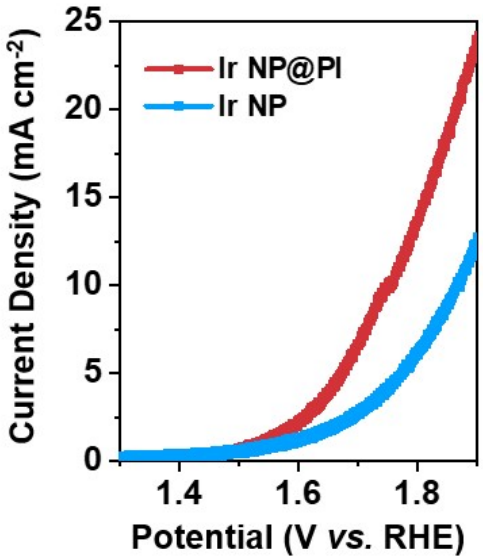

Fig. S9. LSV curves for Ir NP@PI and Ir NP catalysts toward neutral OER catalysis.

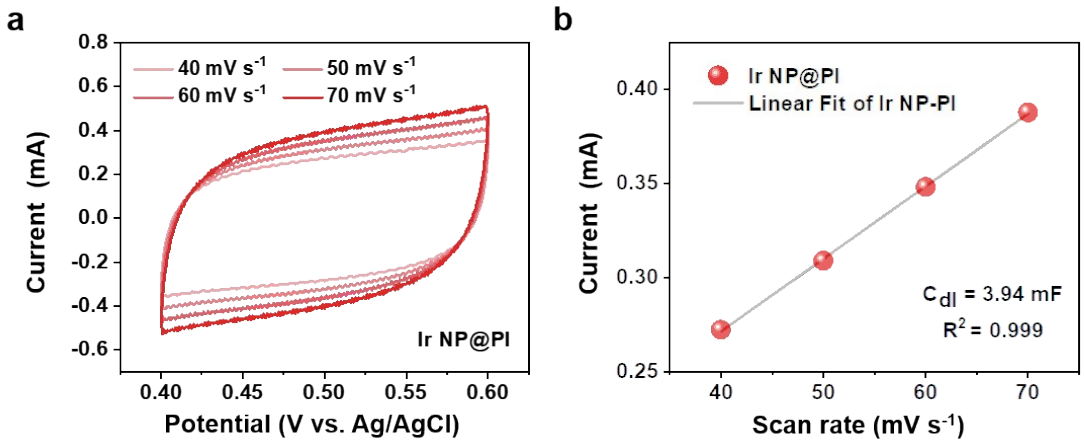

Fig. S10. (a) CV curves for the Ir NP@PI catalyst at scan rates of 40, 50, 60 and 70 mV s^{-1}. (b) Current as a function of scan rate to give the C_{dl} for Ir NP@PI catalyst.

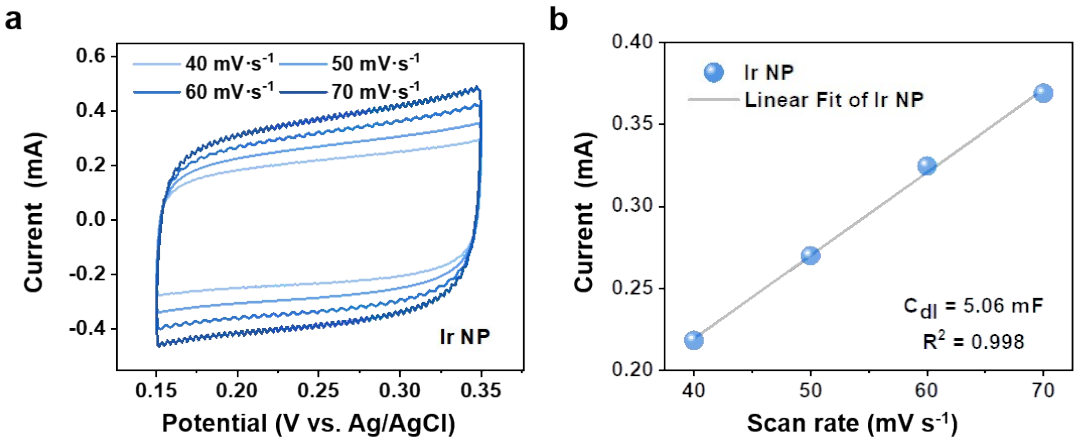

Fig. S11. (a) CV curves for the Ir NP catalyst at scan rates of 40, 50, 60 and 70 mV s^{-1}. (b) Current as a function of scan rate to give the C_{dl} for Ir NP catalyst.

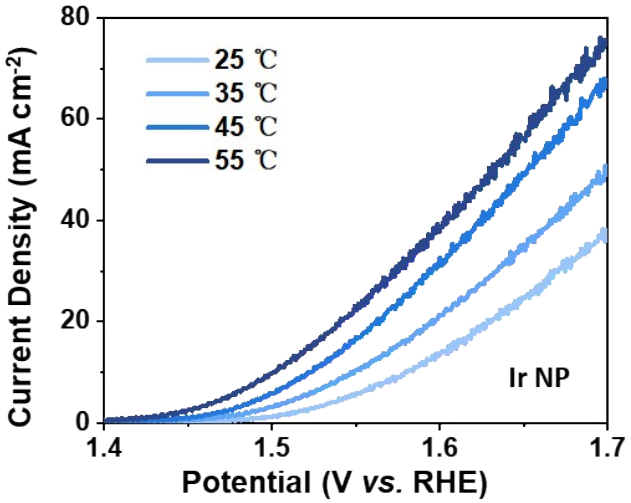

Fig. S12. LSV curves for Ir NP under different temperatures: 25, 35, 45 and 55 ℃.

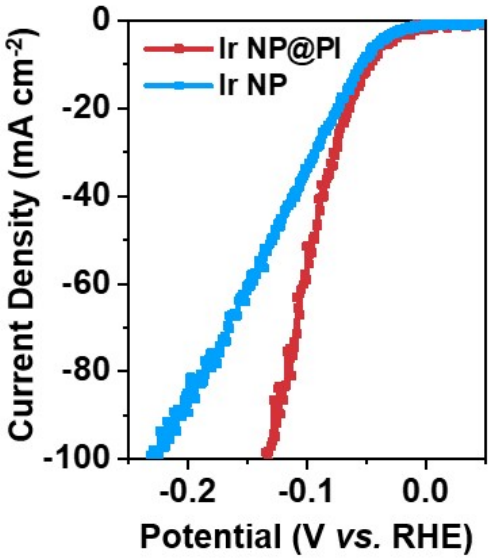

Fig. S13. LSV curves for Ir NP@PI and Ir NP catalysts toward acidic HER catalysis.

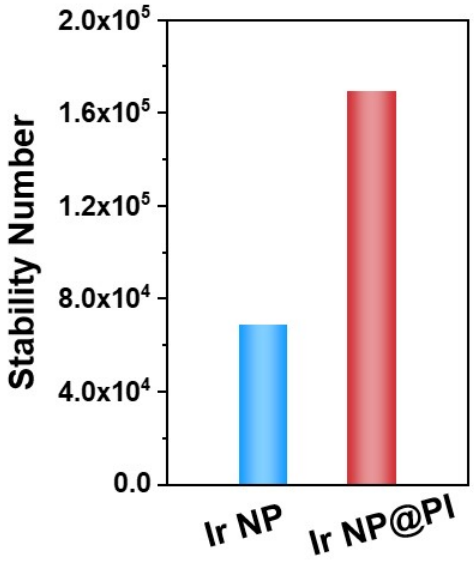

Fig. S14. The calculated stability number for Ir NP@PI and Ir NP electrodes.

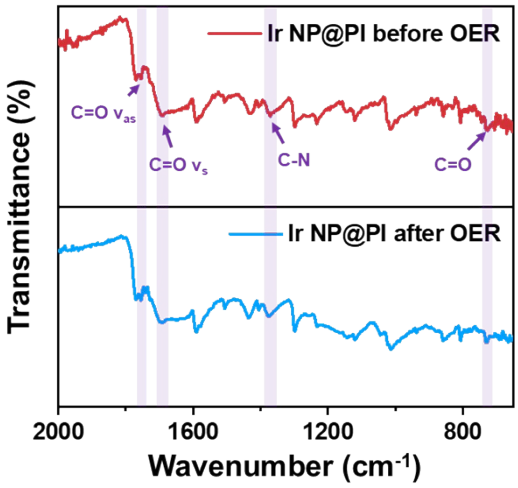

Fig. S15. FTIR spectra for Ir NP@PI catalyst before and after OER catalysis.

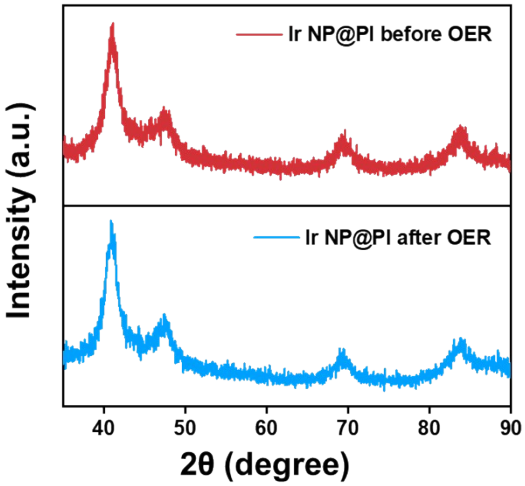

Fig. S16. XRD patterns for Ir NP@PI catalyst before and after OER catalysis.

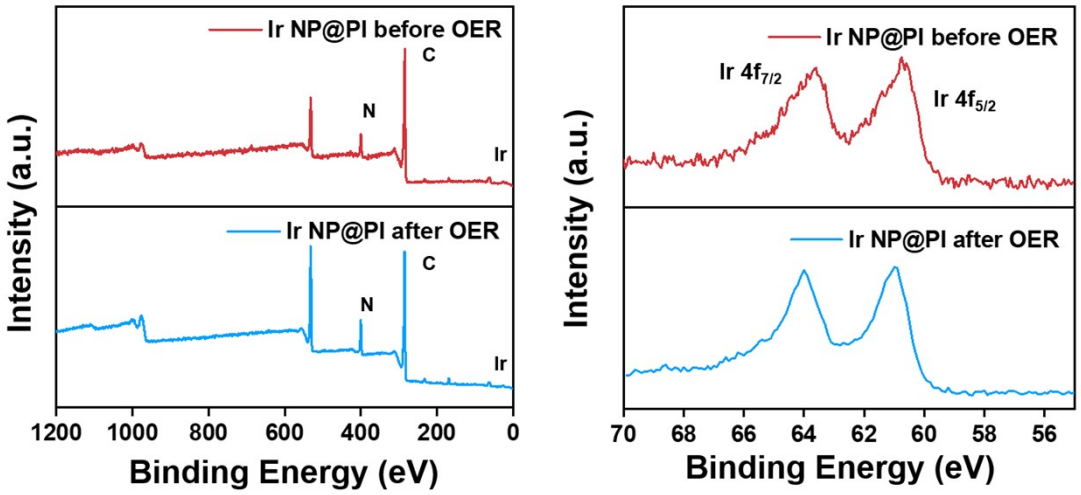

Fig. S17. XPS spectra for Ir NP@PI catalyst before and after OER catalysis.

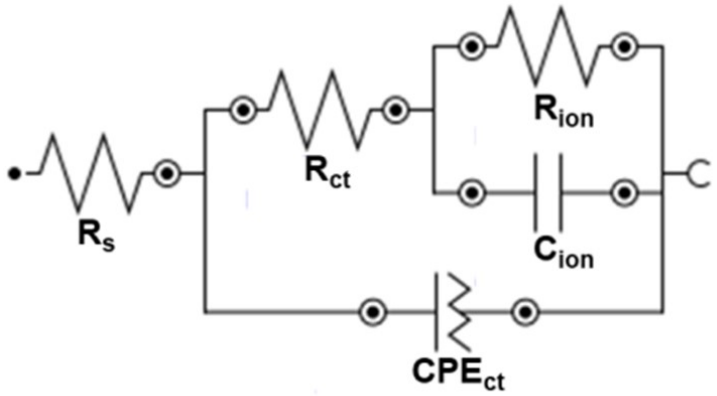

Fig. S18. The equivalent circuit for the simulation. The scattered symbol represents the experimental results, and the solid lines is simulated fitting results.

Table S1. Summary of electrochemical performance of each catalyst on GCEs.

Sample	η^{1} (mV)	C_{dl} (mF)	ECSA (cm^2)	MA[2] ($A\ g^{-1}$)	SA[3] ($mA\ cm^{-2}$)	TOF[4] (s^{-1})
Ir NP@PI	247	3.94	0.11	315.26	25.84	0.16
Ir NP	293	5.06	0.14	27.26	6.73	0.014

[1] Overpotential at 10 mA cm^{-2}.

[2] Calculated according to mass loading of Ir metal atoms. η = 300 mV.

[3] Calculated according to ECSA area. η = 300 mV.

[4] Calculated according to mass loading of Ir active sites. η = 300 mV.

Table S2. Fitting results of in-situ EIS measurements for OER process.

Samples	Potential (V)	R_s (Ω)	R_{ct} (Ω)	CPE_{ct} (F)	R_{ion} (Ω)	C_{ion} (F)
Ir NP@PI	1.25	1.32	2.28	0.783	7.21	0.0228
	1.30	1.27	1.01	0.746	0.753	0.046
	1.35	1.25	0.686	0.763	0.253	0.069
	1.40	1.24	0.528	0.737	0.118	0.088
	1.45	1.26	0.384	0.815	0.093	0.111
Ir NP	1.25	2.09	5.35	0.811	0.072	0.014
	1.30	2.02	1.64	0.805	0.0286	0.0178
	1.35	2.04	0.886	0.78	0.0217	0.0195
	1.40	1.95	0.684	0.711	0.0208	0.0365
	1.45	1.86	0.578	0.701	0.0195	0.045

References

1 Y. Kim, P. P. Lopes, S. Park, A. Lee, J. Lim, H. Lee, S. Back, Y. Jung, N. Danilovic, V. Stamenkovic, J. Erlebacher, J. Snyder and N. M. Markovic, *Nat. Commun.*, 2017, **8**, 1449.

2 M. Risch, K. A. Stoerzinger, T. Z. Regier, D. Peak, S. Y. Sayed and Y. Shao-Horn, *J. Phys. Chem. C*, 2015, **119**, 18903-18910.